A novel approach to biphasic strategy for intensification of the hydrothermal process to give levulinic acid: use of an organic non-solvent

Domenico Licursi[a], Claudia Antonetti[a], Rudy Parton[b], Anna Maria Raspolli Galletti[a*]

[a] *Department of Chemistry and Industrial Chemistry, University of Pisa, Via G. Moruzzi 13, 56124, Pisa, Italy.* [b] *GFB Europe BV, Brightlands Chemelot Campus, Burg. Lemmensstraat 358, 6163JT, Geleen, The Netherlands*

Corresponding author:* anna.maria.raspolli.galletti@unipi.it

Levulinic acid is a platform chemical obtained from acid-catalyzed hydrothermal conversion of cellulose-rich biomass. The low amounts of solid biomass which can be handled in the reactor limit the levulinic acid concentration in the aqueous stream, making the economic viability of the aqueous phase process unsuitable for large scale applications. Now a novel approach to biphasic process has been proposed, where a mineral oil has been used as *non-solvent* for levulinic acid, thus concentrating it in the water phase, reducing the water volume to be processed downstream but at the same time maintaining enough liquid phase to sustain the slurry processability. The work has studied: *i)* the optimization of the biphasic hydrolysis of corn grain to levulinic acid; *ii)* the characterization of the recovered oil; *iii)* the evaluation of the energetic properties of the recovered hydrochar for its exploitation, thus smartly closing the biorefinery cycle.

Keywords: Levulinic acid, hydrothermal process, biphasic hydrolysis, mineral oil, hydrochar.

1. Introduction

Levulinic acid (LA), or 4-oxopentanoic acid, is a C5 keto-carboxylic acid obtained by acid-catalyzed hydrothermal conversion of C6-rich biomasses (Van der Waal and De Jong, 2016; Girisuta and Heeres, 2017). Due to its keto-carboxylic bifunctionality, this versatile molecule was proposed by the US

Department of Energy as one of the most promising and valuable bio-based "*platform chemicals*", exploitable for the synthesis of new bio-derivatives, such as solvents, plasticizers, fuels and oxygenated fuel additives, monomers, etc. (Antonetti et al., 2016; Freitas et al., 2016). The C6-route for LA production was developed on pilot-scale with the Biofine Technology (Hayes et al., 2006), which provided two acid-catalyzed steps, both operating in a continuous mode. This process is attractive, claiming LA yields as high as 70% of the theoretical possible yields, but under industrial conditions (relative high biomass loading), based on the kinetics developed by Girisuta et al. (2007), that is unlikely. Formic acid (FA) is the main reaction co-product, produced generally in equimolar amount respect to LA (Antonetti et al., 2016). Instead, insoluble humins represent the main solid by-products obtained within this process (Filiciotto et al., 2018; Heltzel et al., 2016), deriving from condensation reactions between the furanic intermediates and C5/C6 sugars, and these are separated from the hydrolyzate solution by filtration, after LA production. Subsequent LA isolation from the water phase is generally carried out by solvent extraction, which is subsequently removed and recycled via distillation, whilst LA can be further purified via atmospheric or vacuum distillation and steam stripping, up to a maximum final purity of about 99% (Rijke et al., 2014). From an industrial perspective, this process still maintains important drawbacks, the main consisting of LA recovery from the diluted hydrolysates and the relative low LA concentration per reactor volume and time unit, due to the dilution of solid biomass to allow its processability. Increasing the biomass concentration drops the yields, but from a certain percentage of biomass stirring and processing will not be possible anymore. Moreover, a higher concentration of humins could cause clogging of the piping systems and the reactor. All these drawbacks have limited its technological development at a semi-commercial scale (Silva et al., 2017). GFBiochemicals (2018) has recently developed a new process, introducing significant technological improvements, mainly in the reactor and downstream LA purification. However, process economics is still limited by the low concentration of biomass which can be processed. Currently, biomass loading does not overcome 20 wt%, depending on the type of loaded biomass whereas, at higher concentrations, the slurry is difficultly processable and can cause serious problems of pump plugging. The low biomass concentration limits that of LA in the aqueous solution and, as a consequence, it significantly increases

capital expense (CAPEX) and energy costs of the LA downstream workup. In order to lower the LA production costs, it is necessary to improve its concentration in water phase at the reaction step, as much as possible, developing new alternative solutions. A very interesting solution has been recently proposed by Badainarayana et al. (2016), Kang and Yu (2016) and Rivas et al. (2018), which have increased LA concentration by re-processing the LA mother liquor, thus performing subsequent batches with new biomass. From a different perspective, the use of an extraction solvent in a biphasic system with water can represent a key improvement for the LA productivity, because its extraction would increase the reaction rate, yield, and product quality, at the same time facilitating the downstream LA recovery/concentration and the catalyst recycling. Many solvents have been proposed, including alkylphenols, ketones, alcohols, fatty acids, esters, ethers, halogenated hydrocarbons (Mullen et al., 2013; Kumar et al., 2018), octanol and methyl isobutyl ketone (Nhien et al., 2016a). Moreover, other green and sustainable bio-based extraction solvents have been tested, including γ-valerolactone (Raspolli Galletti et al., 2013; Wettstein et al., 2012), 2-methyltetrahydrofuran (Laitinen et al., 2016), and furfural (Nhien et al., 2016b). However, the use of most of these organic solvents is not sustainable on an industrial scale, due to their low distribution coefficients at the reaction temperature, which lead to large adopted volumes and high costs for their recovery/reuse. This problem has been partially solved adopting tertiary amines as reactive solvents, in particular, tri-*n*-octylamine, together with diluents, such as isoamyl alcohol, hexan-1-ol, octan-1-ol, nonan-1-ol, and methyl isobutyl ketone (Kumar et al., 2011). In many of the abovementioned cases, the organic solvent is added after the hydrolysis reaction to LA, rather than being added “in-situ“, together with the starting reaction mixture. Furthermore, many other problems have not been tackled in the literature, in particular *i)* the possibility of co-extracting the acid catalyst, which should be further separated and recycled, *ii)* the thermal and chemical stability of the organic solvent, which is generally underestimated, but is otherwise very important, especially from an industrial perspective.

A possible innovative solution to improve the LA concentration in the aqueous hydrolysate, and therefore to reduce costs in the recovery section and potentially to increase biomass concentration in the reactor, could be the use of an organic “*anti-solvent*“ in a biphasic system with water. The optimum

anti-solvent should be: *i)* completely insoluble in water, *ii)* selectively unfavorable for the LA extraction, but providing enough liquid volume for maintaining the reactivity/processability of the reactive slurry, and *iii*) not reactive under the reaction conditions. This should result in a significant increase of the final LA concentration into the water phase, thus leading to significant economic savings in the downstream purification operations. This smart idea has been reported in this work for the first time, adopting a traditional white paraffin oil as organic phase. Its high availability, low-cost, safe handling and thermal stability are just a few of the features that make it already very attractive for many industrial applications (Speight, 2015). In this work, the acid-catalyzed hydrothermal conversion of corn grain in a biphasic [mineral oil/water] system was studied and compared with that related to the traditional monophasic path, evaluating if and how the catalytic performances, in terms of glucose conversion, LA/FA yield and LA/FA selectivity, in the aqueous phase, are affected by the presence of this anti-solvent. Dilute sulfuric acid was chosen as the homogeneous catalyst, thanks to its well-known high catalytic activity towards LA and to its low-cost. The investigation was focused on the verification of the feasibility of this reaction, moreover evaluating the effect of the acid concentration, agitation speed, and oil recycle on the LA/FA production, in the perspective of a real optimization of the reaction. Furthermore, a complete characterization of the recovered mineral oil was carried out, in order to demonstrate its physicochemical stability and further justify this innovative approach.

2. Materials and Methods

2.1. Materials

Milled corn grain was provided by GFBiochemicals, Caserta (CE), Italy, which has got it from a farm located in the neighbourhood of the LA demo plant, and used as-received for the hydrolysis tests. White mineral oil (BFRO70, *Paraffinum Liquidum*, FU) was purchased by A.C.E.F. S.p.A., Piacenza, Italy. Sulfuric acid (ACS reagent, 95-98 % purity) was purchased by Sigma-Aldrich and used as-received, as well as levulinic acid (RPE grade, 98 % purity). Formic acid (RPE grade, 99% purity) was purchased by Carlo Erba and used as received.

2.2. Methods

2.2.1. Compositional analysis of corn grain

The compositional analysis of the adopted corn grain, which includes moisture, ash, ethanol-soluble extractives, structural carbohydrates (cellulose and hemicelluloses), and acid-insoluble (Klason) lignin content, was carried out on the basis of the standard NREL procedures (Sluiter et al., 2008a, 2008b, 2008c, 2005).

2.2.2. Monophasic and biphasic hydrolysis experiments

The hydrolysis reaction was carried out in a 600 mL Parr zirconium-made fixed head autoclave (grade 702: Zr + Hf: 99.2 % min., Hf: 4.5 % max). Maximum allowed operating conditions for the autoclave were: temperature: 350 °C, pressure: 65 bars. The autoclave was controlled by means of a Parr Controller 4848. The reactions were carried out at the fixed temperature of 190 °C, for 1 hour, under autogenous conditions. Biphasic reactions were carried out at different agitation speeds, e.g. without any stirring, at 250 and at 500 rpm, by means of a pitched blade turbine impeller. A pressure transducer and an internal thermocouple allowed the monitoring of the internal pressure and temperature of the autoclave. At the end of the hydrolysis reaction, the slurry was filtered on a Büchner funnel, adopting a separatory funnel for the collection of the filtered (water + oil) suspension, and recovering the hydrochar on the filter. A T-shape joint was used between the Büchner funnel and the separatory one, and this system was connected to a membrane pump, in order to speed up and improve the filtration procedure, due to the oil viscosity. First of all, the aqueous phase was separated and, subsequently, the mineral oil, both from the bottom of the separatory funnel. This latter was subsequently decanted, in order to completely remove any coarse water drops deriving from the residual aqueous phase. Regarding the separated hydrochar, this was dried at 105 °C for 24 h and stored in a desiccator. Furthermore, about 5 grams of the water-dried hydrochar were weighed in a Whatman cellulose extraction thimble and extracted with hexane in a traditional Soxhlet apparatus, maintaining the solid/liquid extraction for about 45 hours. At the end of the procedure, the extraction thimble with the residual hydrochar was

dried up to constant weight under vacuum, by using a rotary vane oil-sealed mechanical pump. Extraction yield (%) was calculated as follows:

Extraction Yield (%)=100–[(Dried residual hydrochar (g)/dried starting hydrochar (g)) x 100] (1)

2.2.3. Quantitative determination of LA and FA in the aqueous phase

Quantitative determination of LA and FA was carried out by High Performance Liquid Chromatography (HPLC), adopting a Perkin Elmer Flexar Isocratic Platform, equipped with a column Benson 2000-0 BP-OA (300 mm × 7.8 mm), which was kept at 60 °C, and employing 0.005 M H_2SO_4 as mobile phase (flow rate, 0.6 mL/min). Calibration curves were acquired by adopting commercial standards of LA and FA. At least three replicates for each concentration of standard were carried out, as well as of the real hydrolysate solutions, obtaining a reproducibility within 3%. LA/FA yield was calculated on a molar basis, as follows:

LA Yield (mol%)=[LA in water phase (mol)/glucose in starting formulation (mol)] x 100 (2)

FA Yield (mol%) = [FA in water phase (mol)/glucose in starting formulation (mol)] x 100 (3)

Instead, glucose conversion was calculated as follows:

Glucose conversion (mol%) = [(mol glucose (t_0) – mol glucose (t_{1h}))]/mol glucose (t_0)] x 100 (4)

Lastly, LA and FA selectivities were calculated as follows:

LA selectivity (mol%) = [LA Yield (mol%)/Glucose conversion (mol%)] x 100 (5)

FA selectivity (mol%) =[FA Yield (mol%)/Glucose conversion (mol%)] x 100 (6)

2.2.4. Physical properties of the mineral oil

The following physical properties of the starting and recovered mineral oil were determined on the basis of the ASTM methods (Copeland, 2010), and compared: carbon residue, density at 15 °C, viscosity at 40 °C, number of acidity (as "Total Acid Number", TAN), color, distillation characteristics at atmospheric pressure, and water content. Lastly, the thermal stability of the starting/recycled mineral oil was evaluated by differential scanning calorimetry (DSC). Calorimetric measurements were carried out with a TA 8000/DSC 820 (Mettler-Toledo, Switzerland), setting up the following experimental conditions: 5 °C/min. as heating rate, and 30-300 °C as overall temperature range, and working under static air.

2.2.5. FT-IR and UV-Vis analyses

Fourier Transform-Infrared (FT–IR) characterization of mineral oils and hydrochar was performed with a Perkin-Elmer Spectrum-Two spectrophotometer, equipped with an Attenuated Total Reflectance (ATR) apparatus. The acquisition of each spectrum has provided 12 scans with a resolution of 8 cm^{-1}, in the wavenumber range between 4000 and 450 cm^{-1}. UV-Vis spectra of the mineral oil samples were acquired with a double beam Jasco V-750 spectrometer, within the range 215-600 nm, after appropriate dilution of the samples in hexane.

2.2.6. Chromatographic analyses of the mineral oil

1 mL of the recovered mineral oil was extracted three times by addition of 600, 400 and 400 μL of basified water (pH~9), in order to shift the partition of the salified compounds into the water phase. After separation of the aqueous phase, this was acidified by addition of 1 mL of HCl 6 N and directly analyzed by HPLC for the detection of LA, FA, and other reaction products deriving from the hydrolysis reaction (according to the analytical method already reported in paragraph 2.2.3.). In addition, the acidified aqueous phase was extracted three times (600, 400 and 400 μL, respectively) with Et_2O, and the overall extract was analyzed by Gas Chromatography/Mass Spectrometry (GC/MS) for the detection of the compounds of interest. Gas-chromatographic separation was carried out by a

chemically bonded fused-silica capillary column HP-5MS (Agilent Technologies, Palo Alto, CA, USA), stationary phase 5% phenyl–95% methylpolysiloxane (0.25 mm internal diameter, 0.25 μm film thickness, 30 m length). The carrier gas was helium (99.995% purity), at a constant flow of 1.2 mL/min. The adopted chromatographic conditions for the separation of the silylated compounds were the following: starting temperature 50 °C, isothermal for 1 min., 3 °C/min. up to 250 °C, lastly isothermal for 5 min. Chromatograms were acquired in TIC (Total Ion Current, mass range 20–800) mode. 7890N GC system gas chromatograph (Agilent Technologies), which was coupled with a 5977 mass selective detector (Agilent Technologies) single quadrupole mass spectrometer, was used. The GC was equipped with a split/splitless injector, working at 250 °C, and the injection of the sample was done in splitless mode. The mass spectrometer was operated in the EI positive mode (70 eV). The MS transfer line temperature was 280 °C, the MS ion source temperature was kept at 230 °C, and the MS quadrupole temperature was kept at 150 °C.

Regarding the evaluation of the chemical stability of the recovered mineral oil, the hydrocarbons profile was qualitatively checked by GC/MS technique and compared with that of the untreated oil. For this purpose, about 3 mg of oil were dissolved in 1 g of isooctane, and 2 μL of the diluted sample were injected into the GC/MS system. For this analysis, the same above-reported GC/MS instrumentation and experimental conditions were adopted, except for the temperature of the injector, which was set up at 280 °C, and for the adopted chromatographic conditions, which were the following: starting temperature 80 °C with isotherm for 2 min., then 10 °C/min. up to 200 °C, and isotherm for 3 min., then 10 °C/min. up to 280 °C, and isotherm for 3 min., then 20 °C/min. up to 300 °C, and isotherm for 30 min. Also in this case, chromatograms were acquired in TIC (mass range 20–800) mode.

2.2.7. Elemental analysis and energetic properties of the hydrochar

Elemental analysis (C, H, N, S) of starting corn grain and hydrochar was performed by an automatic analyzer Vario MICRO Cube. These elements were quantified adopting a thermal conductivity detector (TCD). Lastly, oxygen content was calculated by difference: O (%) = 100 (%) – C (%) – H (%) – N (%) – S (%). Determination of Higher Heating Value (HHV) of the starting biomass and hydrochar was

carried out adopting an automatic LECO AC 500 calorimeter. Further details about the experimental procedure have been reported in a previous work (Licursi et al., 2016).

Lastly, energy densification ratio and energy yield (%) have been calculated, as follows:

$$\textit{Energy densification ratio} = \textit{HHV of dried hydrochar/HHV of dried raw biomass} \quad (7)$$

$$\textit{Energy yield (\%)} = \textit{hydrochar yield (\%)} \times \textit{energy densification ratio} \quad (8)$$

where hydrochar yield is calculated on mass basis, as follows:

$$\textit{Hydrochar yield (wt\%)} = [\textit{dried hydrochar recovered (g)} / \textit{dried starting corn grain (g)}] \times 100 \quad (9)$$

3. Results and Discussion

3.1. Monophasic versus biphasic approach: Results

The starting corn grain feedstock was characterized in term of structural carbohydrates, lignin, extractives, and ash content (glucans = 68.29 ± 0.10; xylans = 3.00 ± 0.01; arabinans = 1.45 ± 0.01; acetyl groups = 0.23 ± 0.04; acid-insoluble (Klason) lignin = 3.33 ± 0.30; ethanol-soluble extractives = 9.13 ± 0.08; ash = 1.13 ± 0.03; moisture = 13.48 ± 0.12). Both the high content of glucans and the low one of lignin make the corn grain an excellent feedstock for the verification of the feasibility of this approach, showing a greater availability to the hydrolysis respect to more complex lignocellulosic biomasses (Antonetti et al., 2015). Furthermore, the choice of corn grain as starting feedstock is certainly appropriate, due to its high availability and low price (Silva et al., 2017).

The catalytic performances to LA and FA of the biphasic experiments were evaluated and compared with those of the monophasic ones, e.g. taking into account glucose conversion, LA/FA yield, and selectivity. Experiments have been carried out at fixed reaction temperature (190 °C), time (1 hour), biomass loading (14 wt%), and water/oil ratio (~0.6-0.7), thus changing only the H_2SO_4 concentration in the reaction mixture (1-3 wt%). The results of the investigation are reported in Table 1:

Table 1, near at here

In the monophasic experiments (Exp. 1-3, Table 1), the best catalytic performances have been achieved adopting H_2SO_4 3 wt% (Exp. 3, Table 1). In fact, in this case, the measured LA yield approaches about 45 mol%, which approximately corresponds to the maximum LA yield achievable, e.g. ~50 mol% (Li et al., 2016). In all the performed monophasic experiments, FA is produced in almost equimolar amount respect to LA, in agreement with the stoichiometry of the hydrolysis reaction (Antonetti et al., 2016). Regarding the biphasic experiments (Exp. 4-6, Table 1), the acquired data are very interesting and promising, approaching a maximum LA and FA yield of about 38 and 40 mol%, respectively, with H_2SO_4 3 wt% (Exp. 6, Table 1). However, for the other biphasic experiments (Exp. 4 and Exp. 5, Table 1), glucose conversion is ahead respect to the corresponding monophasic experiments (Exp. 1 and Exp. 2, respectively, Table 1), and the most significant gain, in terms of conversion, LA/FA yield, and selectivity, has been obtained adopting an acid concentration of 2 wt% (Exp. 5, Table 1), which therefore represents the "optimum" condition. In order to clarify the next discussion, the above LA and FA data can be expressed on mass and concentration basis, both referred to the aqueous phase. These data are reported in Table 2:

Table 2, near at here

The above-reprocessed data show that a real concentration of the target compounds in the aqueous phase has been concretely achieved, thus confirming the validity of our approach, mainly aimed at increasing the LA and FA concentration into the aqueous phase.

Taking into account that mineral oil is proposed as an organic "anti-solvent" for the concentration of LA/FA in the aqueous phase, therefore as "inert" diluent, a more accurate comparison of the catalytic performances between the two systems should also take into account that the real concentration of H_2SO_4 is related only to the aqueous phase, rather than including also the oil contribute. On this new mass basis, the real concentration of the acid catalyst in the aqueous phase for the biphasic runs is doubled respect to that in the monophasic ones, but the catalytic performances are not correspondingly preserved in the same way (Exp. 4 and Exp. 2, Table 1). The lower catalytic efficiency of H_2SO_4 in the biphasic runs could be due to an inefficient mass transfer during the biphasic hydrolysis, which is caused by the not optimal autoclave stirring during the hydrolysis reaction. Regarding this aspect, the

solid-liquid phase catalytic reaction system between the biomass and the aqueous water solution may suffer from severe mass transfer limitations that affect the apparent physical reaction rates. The increase of the agitation speed might increase the contact area of the two phases, thus influencing the physical rate processes on a different scale of operation and equipment, by removal of the interfacial mass transfer resistance (Peng et al., 2010). In order to exclude problems related to the solid/liquid mass transfer, the biphasic experiments, which have been already carried out at 250 rpm, were repeated by doubling the agitation speed, and, furthermore, in the complete absence of agitation. The acquired data are reported in Figure 1:

Figure 1, near at here

All the above data confirm that the catalytic performances of the investigated biphasic hydrolysis are almost independent of the agitation speed, thus showing no mixing sensitivity. This is a clear indication that corn grain hydrolysis occurs by fast mass transfer rates compared to the chemical reaction rate or, alternatively, that the mass transfer resistance at the interface of the solid/liquid phase is negligible. The subsistence of the best LA and FA selectivity data, even under the complete absence of agitation, highlights that the intrinsic chemical reaction rates and the mixing rate of the reactants are both fast. On this basis, the biphasic reaction could be carried out adopting simpler technological solutions, thus allowing economic benefits at the next pilot/industrial scale. The overall reduced yield of LA is due to increased sugar concentration in the aqueous phase.

The biphasic experiment with H_2SO_4 2 wt% was still considered as the best one, and therefore the mineral oil recovered from this hydrolysis test (Exp. 5, Table 1) was re-used in subsequent hydrolysis cycles. However, the complete oil recycling between a test and the next one was not realistically feasible, because of unavoidable mass losses occurred as a consequence of the two unit operations, e.g. the unloading of the autoclave and the solid/liquid filtration, this latter being coupled with the liquid-liquid separation. Indeed, about 80 wt% of the starting oil was recovered from each biphasic test, whilst the remaining 20 wt% was introduced as fresh oil, thus realizing a partial recycling. The results of the first five recycling cycles are reported in Figure 2:

Figure 2, near at here

298 The recycling tests confirm the high reproducibility of the catalytic performances to LA/FA (Exp. 5,
299 Table 1, as a test of reference), even after 5 cycles, thus making advantageous and concretely feasible
300 the oil recycling, a mandatory requirement from the industrial scale perspective. At this level of
301 investigation, it is possible to assert that no accumulation of LA/FA into the oil phase has occurred,
302 confirmed by the high repeatability of the catalytic performances respect to the "zero" experiment (Exp.
303 5, Table 1), thus indirectly confirming the role of the mineral oil as inert diluent towards LA and FA.
304 Furthermore, this conclusion has been independently confirmed by the characterization of the recovered
305 mineral oil, which will be discussed in more in depth in the next paragraph.
306 LA is a stable organic acid in the acid aqueous medium, up to a concentration of 500 g/L (Kang and Yu,
307 2016). The good LA stability can be smartly exploited to maximize the intensification of the
308 investigated biphasic reaction. In fact, from an industrial perspective, the synthesized LA could be
309 partially recycled and mixed together with the fresh slurry, thus further improving its final concentration
310 in the aqueous stream. This possibility has been evaluated by introducing LA and FA directly together
311 with the starting reaction mixture, thus simulating their partial recycling, as occurs in the industrial
312 reality. The formulations and the results of these biphasic tests are reported in Table 3:
313 Table 3, near at here
314 The above data evidence that is certainly possible to further increase (respect to the experiment of
315 reference, e.g. Exp. 5, Table 2) the amount of LA/FA in the aqueous phase, by introducing small
316 amounts of these targeted compounds directly as components of the starting formulation. However, LA
317 and FA mass losses significantly increase with the use of progressively higher amounts of these acids
318 and, therefore, their final concentrations in the aqueous phase could certainly be increased, but at
319 expense of a mass loss. This LA/FA mass loss can be attributed to the inhibition of LA/FA formation at
320 high LA/FA concentrations, as well as to the interactions of LA/FA with the solid humins (Kang and
321 Yu, 2016). As justification of their stability in the reaction medium, the pressure/temperature diagrams
322 of these experiments gave a similar trend to that of reference, and the conversion was almost complete
323 (~99%), as for the reference experiment. On the basis of these data, the best compromise between the
324 added- and the recoverable-amounts of LA/FA was ascertained for the Exp. 7, where the final amount of

LA and FA amounted to about 106 and 48 g/L, respectively. In the other two cases (Exp. 8 and Exp. 9, Table 3), the final LA and FA mass losses are too high, and these choices are not certainly advantageous and efficient. The optimal LA and FA concentrations are well in agreement with those reported by Kang and Yu (2016), corresponding to 105 g/L and 39 g/L, respectively.

3.2. Characterization of the recovered mineral oil

3.2.1. Physicochemical properties of the mineral oil

Mineral oil which was recovered at the end of the best biphasic hydrolysis test (Exp. 5, Table 1) was further characterized for selected physicochemical properties, which are indicative of its good quality (Copeland, 2010; Speight, 2015), e.g. density, water content, total acid number (TAN), viscosity, carbon residue, color, and these were compared with those of the starting untreated mineral oil, considered as the reference. The acquired data are reported in Table 4:

Table 4, near at here

Density, viscosity and carbon residue data of the recovered mineral oil support the idea of the stability/inertness of the mineral oil. Regarding color, it changed from “white” to amber, but this does not necessarily confirm the occurred degradation of the oil, and it could be due to the presence of impurities, as previously stated. In this sense, deterioration of color after submission of the oil to an aging test is sometimes limited but the extent of oil deterioration can be much better measured by the acidity development. In our case, TAN is higher than that of the starting oil, and this can be due to the presence of both oxidation products, or traces of residual sulfuric acid, trapped in the W/O emulsion. The latter conclusion is supported by the unavoidable increase of the water content in the recovered oil, whilst the possible presence of oxidation products will be subsequently discussed in the text.

In order to get further information about the thermal stability of the recovered mineral oil, both DSC and distillation curves were acquired and compared with those of the starting mineral oil sample. The DSC curves of the starting and recovered mineral oil show the presence of a weakly exothermic peak at about 185 and 195 °C, respectively, which confirms the bulk similarity between the two samples, and, indirectly, the thermal stability of the mineral oil, which was hydrothermally processed under the best

reaction conditions to give LA. Therefore, the ascertained exothermic thermal transition is typical of the adopted mineral oil sample, rather than to be a consequence of its hydrothermal degradation. In detail, this thermal transition reveals a beginning of the oil oxidation (Santos et al., 2007) but, differently from bulk oxidative degradations, that measured is not energetically notable (ΔH_{ESO} = -155 J/g and ΔH_{ESO} = -180 J/g for the starting and recovered mineral oil, respectively), thus definitely defining the thermal stability of the adopted mineral oil.

The distillation range for light cuts of petroleum derivatives, such as the white oil used in this work, provides very useful information about physical parameters, such as volatility, evaporation rates, and degradation, the latter quantified as residue remaining after the completion of the evaporation. In our case, this characterization has been carried out in order to confirm the physicochemical stability of the recovered oil. Starting mineral oil has a distillation range between 190 and 364 °C, whilst that of the recovered mineral oil is between 160 and 310 °C, in both cases considering the lowest/highest temperature as that for the start/end of distillation and the decomposition temperature, respectively. The lowest temperature is related to the start of distillation, due to the release of volatiles from the oil matrix, whilst the highest one is indicative of a bulk decomposition of the oil, due to the thermal breaking down or cracking of the paraffinic components (Oyekunle and Susu, 2005). The above figure highlights that the distillation curve of the recovered mineral oil is shifted (respect to the same hydrothermally-untreated sample) to lower temperatures, thus highlighting that some degradation has occurred as a consequence of the hydrothermal processing. However, the similarity of the distillation properties of the two samples is indicative of the thermal stability of the mineral oil, which was recovered after corn grain hydrothermal treatment at 190 °C, for 1 hour. The above tests confirm that mineral oil has maintained the bulk liquid phase during the hydrothermal treatment. Furthermore, the extent of degradation of the investigated mineral oil is given by the amount of residue in the distillation flask at the end of the procedure, which includes mainly heavy liquid products and solid coke. The residue recovered after the end of the distillation is 6 %vol. and 27 %vol. for the starting and recovered mineral oil, respectively, and the collected distillate is given by the complement to 100 (taking into account a measured volume loss of 1 %), e.g. 93 %vol. and 72 %vol. for the starting and recovered mineral oil,

respectively. These data confirm that degradation (e.g. cracking) of the mineral oil has certainly occurred, but this becomes significant only by thermally stressing the oil at much more higher temperatures than that used for the corn grain hydrolysis.

From a different but complementary perspective, pressure/temperature diagrams can be very useful to confirm the thermal stability of the adopted mineral oil, thus further supporting the conclusions deduced from the distillation plots. Temperature/pressure versus time plots of a monophasic (Exp. 3, Table 1) and biphasic (Exp. 5, Table 1) run are reported in Figure 3:

Figure 3, near at here

The above figure shows a gradual and constant variation of the pressure increase during the ramping (heating) time of the monophasic/biphasic runs. Then, the temperature (and, as a consequence, the pressure) trend varies within a limited range (± 3 °C), which is certainly acceptable for a correct experimental execution. In both cases, the maximum achieved pressure falls within a similar range, thus highlighting that the pressure increase is due to the vapor pressure of the water, whilst the oil remains in the liquid phase, thus further confirming the conclusions deriving from the interpretation of the distillation plots. The pressure variation, which is stable for the duration of the biphasic test, can be considered as an index of the thermal stability of the oil (Oyekunle and Susu, 2005). On the other hand, in the monophasic test, the maximum pressure, as well as the minimum one, progressively increases towards higher values, thus indicating that a degradation, albeit limited, of some biomass components and/or synthesized intermediates/products into non-condensable gases has occurred.

3.2.2. FT-IR and UV-Vis analysis of the mineral oil

The thermal/oxidative stability (aging) and the presence of impurities/degradation products in the recovered oil was investigated by FT-IR spectroscopy. Regarding the band assignments, that at 2952 cm^{-1} is due to asymmetric -CH_3 stretching vibrations, whilst those at 2921 and 2852 cm^{-1} to asymmetric and symmetric -CH_2 stretching vibrations, respectively (Lucena et al., 2006). Those at 1459 and 1376 cm^{-1} are ascribed to C-H asymmetric bending vibrations of methyl and methylene groups (Lucena et al., 2006). Then, the absorption band at 1143 cm^{-1} is assigned to C-H symmetric bending vibration of

406 methyl groups. Lastly, the band at 720 cm^{-1} is related to the asymmetric deformations of CH_2 groups of
407 the long paraffinic chains (Lucena et al., 2006). The FT-IR characterization confirms that the recovered
408 mineral oil has maintained almost unaltered its starting chemical structure, and this is a clear sign of its
409 chemical stability. In more detail, the absence of the absorption bands typical of oxygenated
410 compounds, such as those in the regions 3500–3300 cm^{-1}, 2700–2600 cm^{-1}, 1800–1700 cm^{-1}, and
411 1200–1100 cm^{-1}, due to alkylhydroperoxides, dialkyl peroxides, alcohols, carboxylic acids, esters,
412 aldehydes and ketones, all these classes of compounds deriving from the oxidation of the oily matrix
413 (Santos et al., 2007), confirms the chemical stability of the recovered mineral oil, which has not heavily
414 aged and deteriorated. Furthermore, the lack of these absorption bands confirms the absence of other
415 oxygenated compounds which may derive from the hydrothermal treatment of the biomass, such as 5-
416 hydroxymethylfurfural, furfural, polymeric soluble humins, and LA/FA. This conclusion represents a
417 further important confirmation of the validity of our approach, mainly aimed at the concentration of LA
418 and FA into the water phase. Moreover, the absence of the water absorption bands (e.g. 3342, 1640 and
419 686 cm^{-1}) demonstrates the net separation between the two phases, which is highly desirable for the
420 biphasic approach. Lastly, the perfect match between the two IR spectra is a clear evidence of the
421 oxidation stability of the recovered mineral oil, which has undergone a thermal treatment under
422 autogenous conditions (e.g. air atmosphere, without any nitrogen washing of the autoclave). All the
423 above considerations are also for the mineral oil recovered after the fifth recycling test (Figure 2), thus
424 demonstrating the chemical stability of the oil even after a repeated thermal stress.
425 After having verified that no sensible degradation of the oil has occurred, the presence of impurities was
426 further evaluated by UV-Vis spectroscopy. The UV-Vis spectrum of the recovered mineral oil reveals
427 the presence of a significant absorption peak at about 270 nm and a weak shoulder at about 330 nm,
428 both indicating the possible presence of conjugated systems of double bonds (Saha et al., 1999). These
429 can derive from the C-C bonding fracture of the mineral oil, leading to the formation of alkane, alkene
430 (cracking reaction), or to the presence of condensed aromatic structures, in our case of furanic source,
431 formed as a consequence of the acid-catalyzed hydrothermal biomass treatment (Heltzel et al., 2016).
432 The solubilization of the furanic compounds in the mineral oils is a known issue, especially in the field

of the transformers, where the degradation (aging) of the oil is monitored by following the release of furanic impurities deriving from the degradation of cellulose insulation paper (Saha, 2003). In order to confirm the solubilization of the furanic compounds in the mineral oil, a blank experiment [H_2SO_4 2 wt% + water + mineral oil] was carried out, adopting the previously optimized reaction conditions, and the UV-Vis spectrum of the recovered mineral oil was acquired. Unlike from the oil recovered from corn grain hydrolysis, which was yellow, that recovered from the blank reaction remained colorless, giving no significant absorption peaks in the UV-Vis region. Definitely, at this level of investigation, the UV-Vis analysis has revealed the presence of furanic compounds, deriving from the biomass hydrolysis. On the basis of the data obtained by the physicochemical characterization, these compounds can be considered as impurities of the oil, thus don't affecting the bulk properties of the mineral oil.

3.2.3. Chromatographic analyses of the recovered mineral oil

In the adopted [mineral oil/water] biphasic system, LA and FA certainly show a higher compatibility, in term of solubility, towards the polar aqueous phase, favored by the presence of their carbonylic/carboxylic groups. However, the further presence of the non-polar hydrocarbon chain could enable the partial solubilization of these organic acids into the oil phase, which could occur especially at the interface's surfaces of the O/W and W/O emulsions. The two phases, visually distinct, should not interact at the separation interface, in order to avoid the inclusion of these organic acids into the oil phase. In order to complete the characterization work and further confirm its "anti-solvent" behavior, the recovered mineral oil (Exp. 5, Table 1) was further analyzed by GC/MS and HPLC techniques. In this regard, the HPLC analysis of the acidified aqueous extract has confirmed the absence of LA, FA and simple furanic compounds (such as furfural and 5-HMF) in the organic phase, and this statement was further confirmed by GC/MS analysis of the Et_2O extract. Definitely, these chromatographic analyses have confirmed that LA and FA were selectively included only in the aqueous phase.

Lastly, the chemical stability of the recovered mineral oil was qualitatively evaluated by GC/MS analysis, by comparing its TIC with that of the starting untreated mineral oil. In this regard, GC is a very effective tool for evaluating differences in the properties of petroleum products, evaluated on the basis

of the distribution of the detected volatile hydrocarbons, thus simulating the traditional distillation procedure, which has been already carried out on this matrix. Furthermore, it gives important information about the presence oil breakdown products, which generally lead to the formation of more polar compounds with higher molecular weights, resulting in longer retention times during the analysis. TIC of both mineral oil saturated hydrocarbons (MOSHs) results in the presence of broad peaks, that do not allow the identification of the individual compounds, as reported in the literature (Krahforst and Healey, 2018). These broad peaks are due to a huge number of hydrocarbon isomers, which are very similar for boiling points, falling mainly within the C_{20}–C_{30} range. For our aims, this analysis confirms the chemical stability of the recovered mineral oil, whose chromatographic profile perfectly follows that of the starting untreated oil sample. Lastly, the absence of additional peaks in the recovered oil, which could justify to the presence of degradation products deriving from both mineral oil itself and biomass conversion, further confirms all the above statements on the inertness of the mineral oil towards LA and FA.

3.3. Characterization of the hydrochar

Hydrochar is the main waste of this process and its reuse for new applications is strongly encouraged for justifying the sustainability of the entire process (Fang et al., 2018; Licursi et al., 2018). The carbonaceous hydrochar deriving from the monophasic hydrothermal conversion of corn grain is essentially composed of polymeric furanic humins, as reported in the literature (Zhao et al., 2016), and it does not include the lignin contribute, which is mostly absent in the starting biomass. A preliminary characterization of the monophasic- and biphasic-derived hydrochars has been carried out, comparing them to forecast the most suitable exploitation strategy.

3.3.1. FT-IR analysis of the hydrochar

Hydrochar recovered from the best biphasic hydrolysis test (Exp. 5, Table 1) was characterized by FT-IR spectroscopy, and compared with that deriving from the corresponding monophasic test of reference (Exp. 3, Table 1), and with that of the starting untreated biomass. Regarding the starting corn grain, the

487 band assignments of its IR spectrum are widely available in the literature and well summarized by Kizil
488 et al. (2002). In detail: 3000-3600 cm^{-1} is assigned to O-H stretching, 2800-3000 cm^{-1} to CH_2
489 deformation, 1642 cm^{-1} to the water adsorbed in the amorphous regions of starch, 1415 cm^{-1} to CH_2
490 bending and C-O-O stretching, 1335 cm^{-1} to C-O-H bending and CH_2 twisting, 1242 cm^{-1} to CH_2OH
491 (side chain) related mode, 1163 cm^{-1} to C-O, C-C stretching, 1070 cm^{-1} to C(1)-H bending, 930 cm^{-1} to
492 skeletal mode vibrations of α-1,4 glycosidic (C-O-C) linkages, 860 cm^{-1} to C(1)-H, CH_2 deformation,
493 760 cm^{-1} to C-C stretching vibrations, and 537 cm^{-1} to skeletal modes of the pyranose ring.
494 The comparison between the IR spectrum of the starting corn grain and that of the hydrochar recovered
495 from monophasic hydrolysis highlights the important change of the chemical structure of the starting
496 feedstock, achieved as a consequence of the performed hydrothermal treatment. Taking into account the
497 behavior of the solid phase within the hydrothermal treatment, the complete conversion of glucose (Exp.
498 3, Table 1) has led to the formation of carbonaceous humins, which are composed of insoluble
499 polyfurans, with carbonylic and hydroxylic functionalities (Bernardini et al., 2017; Licursi et al., 2017,
500 2015). IR band assignments of the monophasic-derived hydrochar have been reported in the literature
501 (Licursi et al., 2017; Sevilla and Fuertes, 2009). In summary, the broad band around 3300 cm^{-1} is
502 assigned to O-H (hydroxyl or carboxyl) stretching vibration, the peak at 2924 and 2854 cm^{-1} to
503 stretching vibration of the aliphatic C-H. The peak at 1720 cm^{-1} corresponds to C=O stretching
504 vibrations of carboxylic and keto groups, which reveals the presence of these functional groups on the
505 hydrochar surface. The bands at 1605 cm^{-1} and 1515 cm^{-1} are related to ring vibrations of the C=C
506 bonds of the furanic structures, and those in the region 1400–1100 cm^{-1} correspond to C-O-C vibration.
507 Lastly, new absorption bands at 860 cm^{-1} and 800 cm^{-1} are found in the monophasic-derived hydrochar,
508 assigned to aromatic out-of-plane bending vibrations of C-H bonds.
509 Regarding the IR spectrum of the biphasic-derived hydrochar, its absorption bands are much less intense
510 than those of the monophasic-derived one. This is clearly due to the presence of the mineral oil on the
511 hydrochar surface, confirmed by its intense absorption bands at 2952, 2921 and 2852 cm^{-1}, which
512 significantly flatten those belonging to the functional groups of the hydrochar. On this basis, the
513 reactivity of the biphasic-derived hydrochar, considered in terms of free and reactive hydroxyl/carbonyl

514 groups, is much more hampered than that of the monophasic-derived one, and therefore its possible
515 application as adsorbent for environmental applications is not suitable, thus preferring its combustion
516 per energy recovery, mainly as: *i)* immediate combustion of the [hydrochar + trapped mineral oil], or *ii)*
517 preliminary recovery of the mineral oil from the hydrochar by solvent extraction and subsequent
518 combustion of the hydrochar. Both these proposals will be briefly discussed in the next paragraphs.
519
520 **3.3.2. Elemental analysis and energetic properties of the hydrochar**
521 Elemental composition of the investigated samples has been determined, e.g. starting corn grain (45%
522 C, 7.1% H, 1.3% N, 0.1% S, 46.5% O), monophasic- (64.7% C, 5.6% H, 1.2% N, 1.7% S, 26.8% O) and
523 biphasic-derived (75.6% C, 10.3% H, 1.0% N, 0.8% S, 12.3% O) hydrochars. The higher sulfur content
524 of the biphasic-derived hydrochar is due to the presence of some H_2SO_4 residues in the emulsified oil
525 phase, trapped together with the hydrochar, as previously highlighted during the characterization of the
526 recovered mineral oil. These data can be reported as H/C and O/C atomic ratios in the Van Krevelen
527 plot of Figure 4, which gives a good visual representation of the biomass coalification progress (Licursi
528 et al., 2017). In the same figure, H/C and O/C ratios of other biomasses/LA-derived hydrochars of
529 interest are also reported, for comparison purposes.
530 Figure 4, near at here
531 The above data show that, independently from the adopted starting feedstock, the monophasic-derived
532 hydrochars have similar H/C and O/C atomic ratios, falling within those of the traditional Brown coals
533 (Licursi et al., 2017, 2015). Instead, in the case of the biphasic-derived corn grain hydrochar, its O/C
534 ratio falls within the range of the sub-bituminous coals (about 0.1 in both cases), but it has a much
535 higher H/C ratio (about 1.6 for the hydrochar versus 0.8 for the sub-bituminous coals) (Licursi et al.,
536 2017, 2015), due to the contribution of the residual hydrocarbon-rich mineral oil. The much lower H/C
537 ratio of the traditional sub-bituminous coals is due to the prevailing demethanation pathway, which
538 occurs under the harsher reaction conditions of the natural coalification process, instead absent in the
539 case of the hydrochars. From the perspective of the liquid fuels, the chemical composition of the
540 biphasic-derived hydrochar falls within the ranges of the best “ideal” ones, such as traditional crude oil

products (diesel, gasoline and kerosene), or biomass-derived fatty acid ethyl esters (FAEEs) and fatty acid methyl esters (FAMEs) (O' Connor, 2013).

In order to complete the above discussion, the energetic properties of the biphasic-derived hydrochar, in terms of higher heating value (HHV), were determined and compared with those of the monophasic-derived hydrochar and the starting untreated biomass. HHV value of the monophasic-derived hydrochar was 26.6 MJ/kg, much more higher than that of the starting untreated biomass, which was 16.2 MJ/kg and falls within those obtained from hydrothermal treatment of different biomasses (Tag et al., 2018). This increase is due to the occurred concentration of the carbon content (respect to the starting untreated biomass), given by the migration of oxygen and hydrogen mainly into the liquid phase (Licursi et al., 2017). Instead, HHV of the biphasic-derived hydrochar is much higher than those of the traditional hydrochars, amounting to 36,1 MJ/kg, due to the contribute of the residual hydrocarbon-rich oil, as previously stated, thus confirming the promising fuel properties of this bio-waste. Monophasic- and biphasic-derived hydrochars gave 1.6 and 2.2 as energy densification ratios, respectively, and 36.8 and 63.8 % as energy yields, respectively. In the case of the biphasic-derived hydrochar, the energetic advantage (as energy densification ratio) should compensate the modest hydrochar mass yields obtained by the hydrothermal processing of this biomass (23 and 29 wt% for the monophasic- and biphasic-derived hydrochar, respectively). By this way, significantly improved energy yield can be achieved for the biphasic-derived hydrochar, in the range of those deriving from more "favorable-for-hydrochar" lignocellulosic biomasses (Elaigwu and Greenway, 2016, Licursi et al., 2017). Definitely, the traditional energetic approach is particularly advantageous for the biphasic-derived hydrochar, given its higher achievable energy yield. Taking into account that the economics of the LA process is already advantageous if based on the only production of this platform-chemical (Silva et al., 2017), the recovered hydrochar can certainly contribute to lower the LA production costs, e.g. by partially recovering the energy spent for its production within a biorefinery plant.

3.3.3. Recovery of the mineral oil from the hydrochar by solvent extraction

Mineral oil was isolated from the hydrochar by extraction with hexane, in order to evaluate the feasibility of the oil recovery, which is a fundamental requisite for the next development of this approach on industrial scale, if the direct combustion of the [hydrochar + trapped mineral oil] for energy recovery is not the preferred choice. The extraction tests have revealed that the hydrochars have retained almost the same amount of mineral oil, corresponding to about 60 wt% of the weight of the starting water-dried hydrochar. This is an important confirmation of the good reproducibility of the entire procedure, considered an ensemble of the unit operations, which include *1)* the biphasic reaction, *2)* the separation of the hydrochar from the (water + oil) liquid phase by vacuum filtration and *3)* the removal of the mineral oil from the hydrochar by solvent extraction. However, from a larger-scale biorefinery perspective, it should be economically advantageous to recover and reuse within the same LA process only the oil fraction which is separated from the solids, whilst the oil adsorbed in the hydrochar should be immediately used to make energy, e.g. without any further separation step. This energy can be used within the same LA plant and electricity surplus can be sold to the grid.

4. Conclusions

Corn grain acid-catalysed hydrolysis to LA in a biphasic [paraffin oil/water] system was investigated. Paraffin oil was used as a non-solvent towards LA, allowing its selective concentration into the polar water phase. The evaluated catalytic performances were comparable with those of the monophasic route. Inertness and thermo-chemical stability of the recovered oil have been demonstrated. Furthermore, recovered hydrochar has revealed promising energetic properties. The proposed approach represents a smart strategy of process intensification, allowing significant cost reduction for LA clean-up operations. It enlarges the possibilities of performing LA synthesis, in the perspective of its market development as commodity chemical.

Acknowledgements

The authors are grateful to PRIN 2015-Project HERCULES "HEterogeneous Robust Catalysts to Upgrade Low valuE biomass Streams " (code 20153T4REF).

Appendix A. Supplementary data

E-Supplementary data of this work can be found in the online version of the paper.

References

1. Antonetti, C., Bonari, E., Licursi, D., Nassi, N., Raspolli Galletti, A.M., 2015. Hydrothermal conversion of giant reed to furfural and levulinic acid: Optimization of the process under microwave irradiation and investigation of distinctive agronomic parameters. Molecules 20, 21232-21253.
2. Antonetti, C., Licursi, D., Fulignati, S., Valentini, G., Raspolli Galletti, A.M., 2016. New frontiers in the catalytic synthesis of levulinic acid: from sugars to raw and waste biomass as starting feedstock. Catalysts 6, 196-225.
3. Badarinarayana, V., Rodwogin, M.D., Mullen, B.D., Purtle, I., Molitor, E.J., 2016. Process to prepare levulinic acid. US 2016/0122278 A1.
4. Bernardini, J., Licursi, D., Anguillesi, I., Cinelli, P., Coltelli, M.B., Antonetti, C., Raspolli Galletti, A.M., Lazzeri, A., 2017. Exploitation of Arundo Donax L. hydrolysis residue for the green synthesis of flexible polyurethane foams. BioResources 12, 3630-3655.
5. Copeland, C.M., 2010. White mineral oils, in: Rand, S.J. (Ed.), Significance of tests for petroleum petroleum products. ASTM International, Pennsylvania, US, pp. 184-188.
6. Elaigwu, S.E., Greenway, G.M., 2016. Microwave-assisted hydrothermal carbonization of rapeseed husk: A strategy for improving its solid fuel properties. Fuel Process. Technol. 149, 305-312.
7. Fang, J., Zhan, L., Ok, Y.S., Gao, B., 2018. Minireview of potential applications of hydrochar derived from hydrothermal carbonization of biomass. J. Ind. Eng. Chem. 57, 15-21.

8. Filiciotto, L., Balua, A.M., Van der Waal, J.C., Luque, R., 2018. Catalytic insights into the production of biomass-derived side products methyl levulinate, furfural and humins. Catal. Today 302, 2-15.
9. Freitas, F.A., Licursi, D., Lachter, E.R., Raspolli Galletti, A.M., Antonetti, C., Brito, T.C., Nascimento, R.S.V., 2016. Heterogeneous catalysis for the ketalisation of ethyl levulinate with 1,2-dodecanediol: Opening the way to a new class of bio-degradable surfactants. Catal. Commun. 73, 84-87.
10. GFBiochemicals, 2018. http://www.gfbiochemicals.com (accessed 20.01.18).
11. Girisuta, B., Janssen, L.P.B.M., Heeres, H.J., 2007. Kinetic study on the acid-catalyzed hydrolysis of cellulose to levulinic acid. Ind. Eng. Chem. Res. 46, 1696-1708.
12. Girisuta, B., Heeres, H.J., 2017. Levulinic acid from biomass: synthesis and applications, in: Z. Fang, Z., Smith R.L. Jr., R. Qi, X. (Eds.), Production of platform chemicals from sustainable resources. Springer Nature Singapore, pp. 143-170.
13. Hayes, D.J., Fitzpatrick, S., Hayes, M.H.B., Ross, J.R.H., 2006. The Biofine process – Production of levulinic acid, furfural, and formic acid from lignocellulosic feedstocks, in: Kamm, B., Gruber, P.R., Kamm, M. (Eds.), Biorefineries – Industrial processes and products: Status quo and future directions. Wiley-VCH Verlag GmbH & Co. KGaA, Weinheim, Germany, pp. 139-164.
14. Heltzel, J., Patil, S.K.R., Lund, C.R.F., 2016. Humin formation pathways, in: Schlaf, M., Zhang, Z.C. (Eds.), Reaction pathways and mechanisms in thermocatalytic biomass conversion II. Springer, Singapore, pp. 105-118.
15. Kang, S., Yu, J., 2016. An intensified reaction technology for high levulinic acid concentration from lignocellulosic biomass. Biomass Bioenergy 95, 214-220.
16. Kizil, R., Irudayaraj, J., Seetharaman, K., 2002. Characterization of irradiated starches by using FT-Raman and FTIR Spectroscopy. J. Agric. Food. Chem. 50, 3912-3918.
17. Krahforst, K., Healey, E.T., 2018. Unraveling the complexities of upland spilled fuels: Selected case studies, in: Stout, S.A., Wang, Z. (Eds.), Oil spill environmental forensics case studies.

Butterworth-Heinemann (Elsevier), Oxford, UK, pp. 201-238.

18. Kumar, T.P., Vishwanadham, B., Prasanna Rani, K.N., Mallikarjun, M., Basava Rao, V.V., 2011. Reactive extraction of levulinic acid from aqueous solutions with tri-n-octylamine (TOA) in 1-octanol: Equilibria, kinetics, and model development. Chem. Eng. Commun. 198, 572–589.
19. Kumar, S., Ahluwalia, V., Kundu, P., Sangwan, R.S., Kansal, S.K., Runge, T.M., Elumalai, S., 2018. Improved levulinic acid production from agri-residue biomass in biphasic solvent system through synergistic catalytic effect of acid and products. Bioresour. Technol. 251, 143-150.
20. Laitinen, A.T., Penttilä, K.J.T., Kaunisto, J.M., 2016. Physical solvent extraction of levulinic acid from dilute aqueous solution with 2-methyltetrahydrofuran. Sep. Sci. Technol. 51, 465-473.
21. Li, Z.-F., Wang, Z.-W., Xu, H.-Y., Ren, S.-X., Chen, Z., Yang, S.-H., He, X.-F., Yang, Y.-T., Li, S.-Q., Lei, T.-Z., 2016. Production of levulinic acid and furfural from biomass hydrolysis through a demonstration project. J. Biobased Mater. Bioenergy 10, 279-283.
22. Licursi, D., Antonetti, C., Bernardini, J., Cinelli, P., Coltelli, M.B., Lazzeri, A., Martinelli, M., Raspolli Galletti, A.M., 2015. Characterization of the Arundo Donax L. hydrolysis residue from hydrothermal conversion: comparison with technical lignins and application perspectives. Ind. Crops Prod. 76, 1008-1024.
23. Licursi, D., Antonetti, C., Martinelli, M., Ribechini, E., Zanaboni, M., Raspolli Galletti, A.M., 2016. Monitoring/characterization of stickies contaminants coming from a papermaking plant – Toward an innovative exploitation of the screen rejects to levulinic acid. Waste Manag. 49, 469-482.
24. Licursi, D., Antonetti, C., Fulignati, S., Vitolo, S., Puccini, M., Ribechini, E., Bernazzani, L., Raspolli Galletti, A.M., 2017. In-depth characterization of valuable char obtained from hydrothermal conversion of hazelnut shells to levulinic acid. Bioresour. Technol. 244, 880-888.
25. Licursi D., Antonetti, C., Mattonai, M., Pérez-Armada, L., Rivas, S., Ribekini, E., Raspolli Galletti, A.M., 2018. Multi-valorisation of giant reed (Arundo Donax L.) to give levulinic acid and valuable phenolic antioxidants. Ind. Crops Prod. 112, 6-17.
26. Lucena, R., Cárdenas, S., Gallego, M., Valcárcel, M., 2006. ATR-FTIR membrane-based sensor

675 for the simultaneous determination of surfactant and oil total indices in industrial degreasing
676 baths. Analyst 131, 415-421.
677 27. Mullen, B.D., Yontz, D.J., Leibig, C.M., 2013. Process to prepare levulinic acid. US9073841
678 B2.
679 28. Nhien, L.C., Long, N.V.D., Kim, S., Lee, M., 2016a. Design and assessment of hybrid
680 purification processes through a systematic solvent screening for the production of levulinic acid
681 from lignocellulosic biomass. Ind. Eng. Chem. Res. 55, 5180–5189.
682 29. Nhien, L.C., Long, N.V.D., Lee, M., 2016b. Design and optimization of the levulinic acid
683 recovery process from lignocellulosic biomass. Chem. Eng. Res. Des. 107, 126–136.
684 30. O' Connor, P., 2013. A general introduction to biomass utilization possibilities, in:
685 Triantafyllidis, K., Lappas, A., Stöcker, M. (Eds.), The role of catalysis for the sustainable
686 production of bio-oils and bio-chemicals. Elsevier, Amsterdam, The Netherlands, pp. 1-25.
687 31. Oyekunle, L.O., Susu, A.A., 2005. High-temperature thermal stability investigation of paraffinic
688 oil. Pet. Sci. Technol. 23, 199–207.
689 32. Peng, L., Lin, L., Zhang, J., Zhuang, J., Zhang, B., Gong, Y., 2010. Catalytic conversion of
690 cellulose to levulinic acid by metal chlorides. Molecules 15, 5258-5272.
691 33. Raspolli Galletti, A.M., Antonetti, C., Ribechini, E., Colombini, M.P., Nassi, N., Bonari, E.,
692 2013. From giant reed to levulinic acid and gamma-valerolactone: A high yield catalytic route to
693 valeric biofuels. Appl. Energy 102, 157–162.
694 34. Rijke, D.A., Hangx, G.W.A., Parton, R.F.M.J., Engendahl, B., 2014. Process for the isolation of
695 levulinic acid. WO 2014087013 A1.
696 35. Rivas, S., Raspolli Galletti, A.M., Antonetti, C., Licursi, D., Santos, V., Parajó, J.C., 2018. A
697 biorefinery cascade conversion of hemicellulose-free *Eucalyptus Globulus* wood: Production of
698 concentrated levulinic acid solutions for γ-valerolactone sustainable preparation. Catalysts 8,
699 169-185.
700 36. Saha, T.K., Darvcniza, M., Yao, Z.T., 1999. Investigating the effects of oxidation and thermal
701 degradation on electrical and chemical properties of power transformers insulation. IEEE Trans.

Power Del. 14, 1359-1367.

37. Saha, T.K., 2003. Review of modern diagnostic techniques for assessing insulation condition in aged transformers. IEEE Trans. Dielectr. Electr. Insul. 10, 903-917.

38. Santos, J.C.O., Lima, L.N., Santos, I.M.G., Souza, A.G., 2007. Thermal, spectroscopic and rheological study of mineral base lubricating oils. J. Therm. Anal. Calorim. 87, 639-643.

39. Sevilla, M., Fuertes, A.B., 2009. Chemical and structural properties of carbonaceous products obtained by hydrothermal carbonization of saccharides. Chem. Eur. J. 15, 4195-4203.

40. Silva, J.F.L., Grekin, R., Mariano, A.P., Filho, R.M., 2017. Making levulinic acid and ethyl levulinate economically viable: a worldwide techno-economic and environmental assessment of possible routes. Energy Technol. doi:10.1002/ente.201700594.

41. Sluiter, A., Hames, B., Ruiz, R., Scarlata, C., Sluiter, J., Templeton, D., Crocker, D., 2005. Determination of ash in biomass. Laboratory Analytical Procedure (LAP), NREL/TP-510-42622.

42. Sluiter, A., Hames, B., Hyman, D., Payne, C., Ruiz, R., Scarlata, C., Sluiter, J., Templeton, D., Wolfe, J., 2008a. Determination of total solids in biomass and total dissolved solids in liquid process samples. Laboratory Analytical Procedure (LAP), Technical Report NREL/TP-510-42621.

43. Sluiter, A., Hames, B., Ruiz, R., Scarlata, C., Sluiter, J., Templeton, D., Crocker, D., 2008b. Determination of extractives in biomass. Laboratory Analytical Procedure (LAP), Technical Report NREL/TP-510-42619.

44. Sluiter, A., Hames, B., Ruiz, R., Scarlata, C., Sluiter, J., Templeton, D., Crocker, D., 2008c. Determination of structural carbohydrates and lignin in biomass. Laboratory Analytical Procedure (LAP), NREL/TP-510-42618.

45. Speight, J.G., 2015. White oil, in: Speight, J.G. (Ed.), Handbook of petroleum product analysis. John Wiley & Sons, Hoboken, New Jersey, pp. 207-221.

46. Tag, A.T., Duman, G., Yanik, J., 2018. Influences of feedstock type and process variables on hydrochar properties. Bioresour. Technol. 250, 337-344.

47. van der Waal, J.C., de Jong, E., 2016. Avantium chemicals: The high potential for the levulinic product tree, in: de María, P.D. (Ed.), Industrial biorenewables: A practical viewpoint. John Wiley & Sons, Hoboken, USA, pp. 97-120.
48. Wettstein, S.G., Alonso, D.M., Chonga, Y., Dumesic, J.A., 2012. Production of levulinic acid and gamma-valerolactone (GVL) from cellulose using GVL as a solvent in biphasic systems. Energy Environ. Sci. 5, 8199-8203.
49. Zhao, M., Li, B., Cai, J.-X., Liu, C., McAdam, K.G., Zhang, K., 2016. Thermal & chemical analyses of hydrothermally derived carbon materials from corn starch. Fuel Process. Technol. 153, 43-49.

Captions for Figures

Figure 1: Effect of the agitation speed on the catalytic performances of the corn grain biphasic hydrolysis in the [mineral oil/water] system, adopting different H_2SO_4 concentrations. **Formulation**: Biomass loading = 14 wt%. **Reaction conditions**: hydrolysis temperature = 190 °C; hydrolysis time = 1 hour.

Figure 2: Recycling tests of the recovered mineral oil (Exp. 5, Table 1, as direct run).

Figure 3: Plots of temperature/pressure versus time for a monophasic (Exp. 3, Table 1) and a biphasic (Exp. 5, Table 1) run.

Figure 4: van Krevelen diagram of the investigated corn grain (starting biomass) and its monophasic- and biphasic-derived hydrochars recovered after LA production. For comparison purposes, other starting biomasses/hydrochars have been included (adapted from (Sevilla and Fuertes, 2009)).

Captions for Tables

Table 1: Monophasic versus biphasic approach: results. **Formulation**: Biomass loading = 14 wt%. **Reaction conditions**: hydrolysis temperature = 190 °C; hydrolysis time = 1 hour; agitation speed = 250 rpm.

Table 2: Mass and concentration data of LA and FA in the aqueous phase, for the monophasic/biphasic hydrolysis experiments. **Formulation**: Biomass loading = 14 wt%. **Reaction conditions**: hydrolysis temperature = 190 °C; hydrolysis time = 1 hour; agitation speed = 250 rpm.

Table 3: Mass and concentration data of LA and FA in the aqueous phase, for the biphasic hydrolysis tests which have been carried out in the presence of LA and FA, both directly introduced in the starting reaction mixture. **Formulation**: Biomass loading = 14 wt%, H_2SO_4 = 2 wt%. **Reaction conditions**: hydrolysis temperature = 190 °C; hydrolysis time = 1 hour; agitation speed = 250 rpm.

Table 4: Physicochemical properties of the starting and recovered (Exp. 5, Table 1) mineral oil.

List of Figures

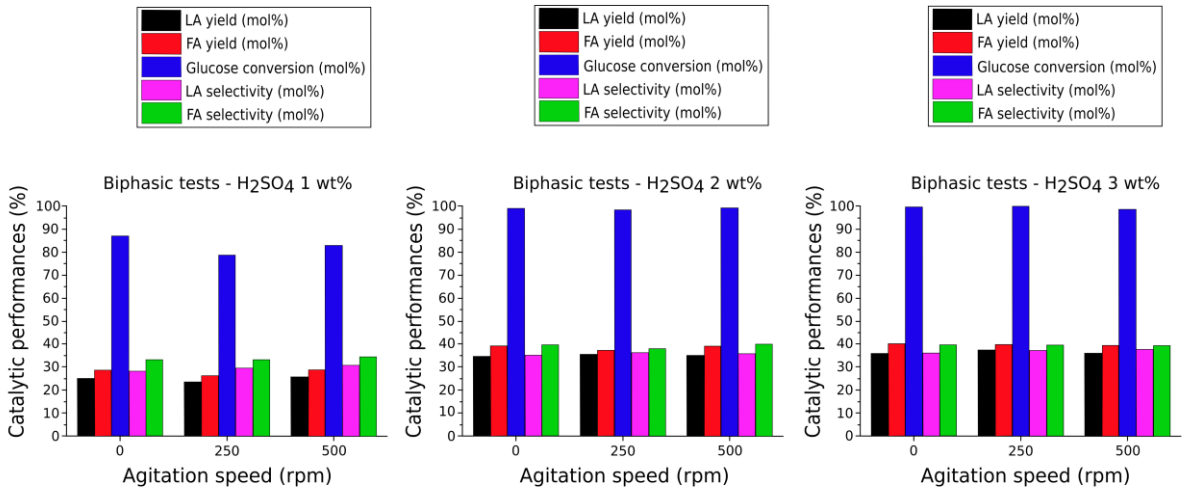

Figure 1

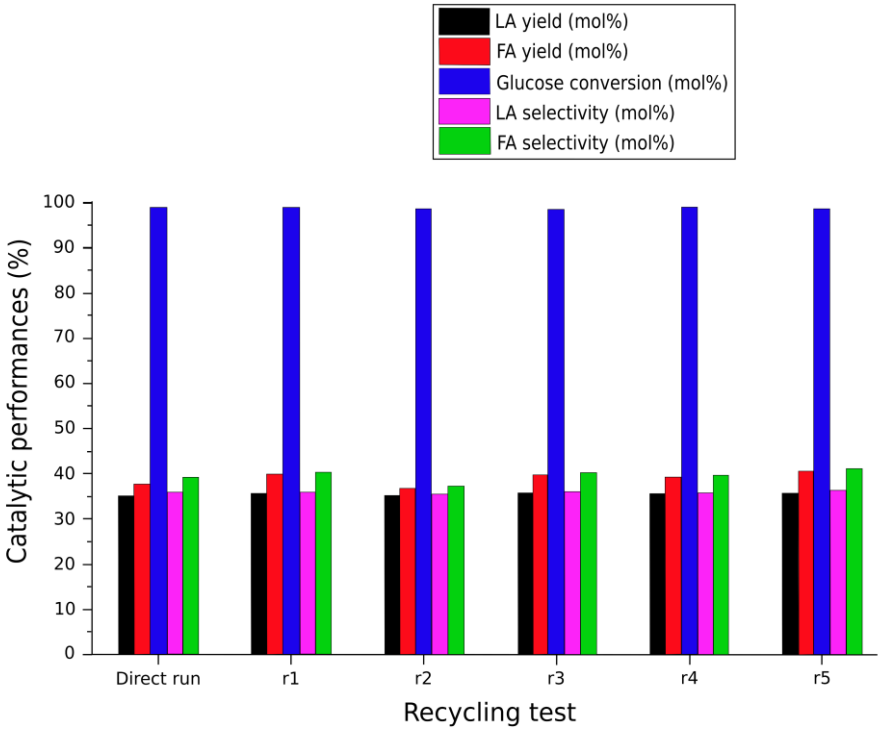
LA yield (mol%)
FA yield (mol%)
Glucose conversion (mol%)
LA selectivity (mol%)
FA selectivity (mol%)
Catalytic performances (%)
0
10
20
30
40
50
60
70
80
90
100
Direct run
r1
r2
r3
r4
r5
Recycling test

Figure 2

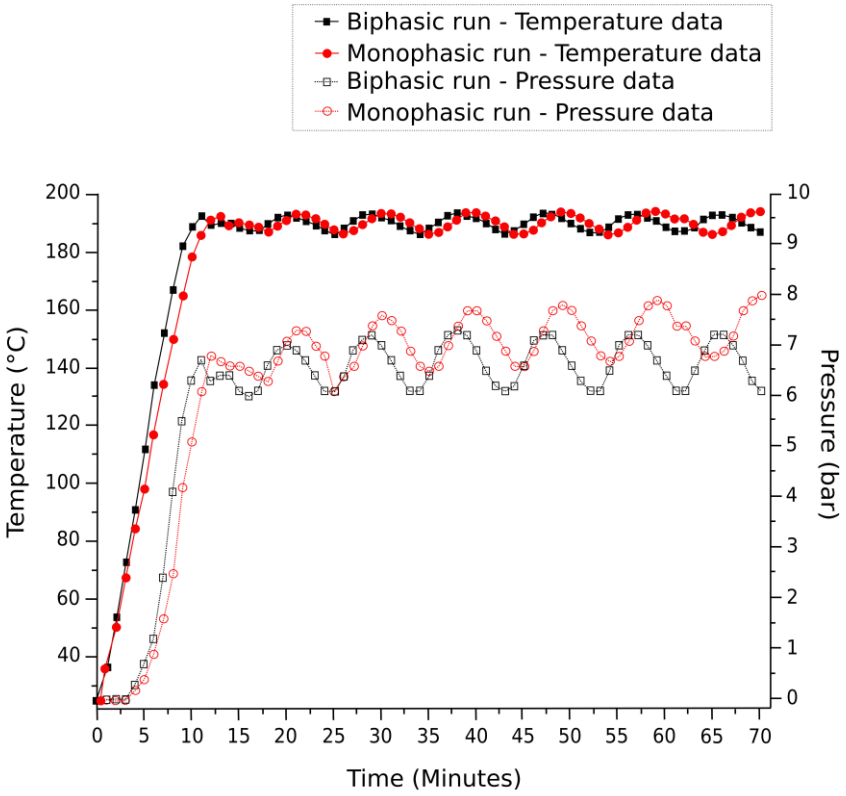
Biphasic run - Temperature data
Monophasic run - Temperature data
Biphasic run - Pressure data
Monophasic run - Pressure data
Temperature (°C)
Pressure (bar)
Time (Minutes)
200
180
160
140
120
100
80
60
40
10
9
8
7
6
5
4
3
2
1
0
0
5
10
15
20
25
30
35
40
45
50
55
60
65
70

Figure 3

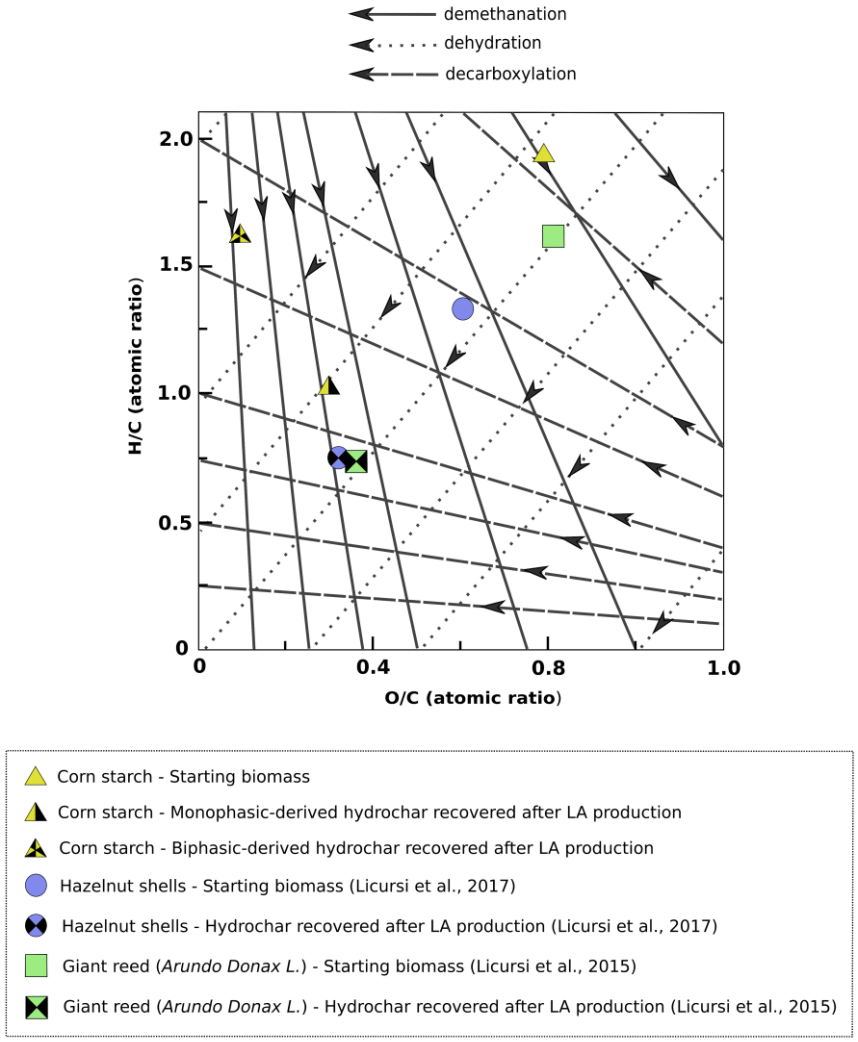
demethanation
dehydration
decarboxylation
H/C (atomic ratio)
O/C (atomic ratio)
2.0
1.5
1.0
0.5
0
0.4
0.8
1.0
Corn starch - Starting biomass
Corn starch - Monophasic-derived hydrochar recovered after LA production
Corn starch - Biphasic-derived hydrochar recovered after LA production
Hazelnut shells - Starting biomass (Licursi et al., 2017)
Hazelnut shells - Hydrochar recovered after LA production (Licursi et al., 2017)
Giant reed (Arundo Donax L.) - Starting biomass (Licursi et al., 2015)
Giant reed (Arundo Donax L.) - Hydrochar recovered after LA production (Licursi et al., 2015)

Figure 4

List of Tables

Table 1

Exp.	Water (wt%)	Mineral oil (wt%)	H_2SO_4 (wt%)	LA yield (mol%)	FA yield (mol%)	Glucose conversion (mol%)	LA selectivity (mol%)	FA selectivity (mol%)
1	85	-	1	13.2	13.7	58.2	22.7	23.5
2	84	-	2	35.4	35.8	85.1	41.6	42.1
3	83	-	3	44.5	44.9	100.0	44.5	44.9
4	33	52	1	23.8	26.5	79.0	30.1	33.5
5	33	51	2	35.3	37.1	97.7	36.1	38.0
6	33	50	3	37.7	39.8	100.0	37.7	39.8

Table 2

Exp.	Water (wt%)	Mineral oil (wt%)	H_2SO_4 (wt%)	LA (g)	FA (g)	LA (g/L)	FA (g/L)
1	85	-	1	0.9	0.4	10.4	4.3
2	84	-	2	2.4	1.0	27.8	11.1
3	83	-	3	3.0	1.2	34.5	14.0
4	33	52	1	1.7	0.8	49.7	22.8
5	33	51	2	2.4	1.0	67.9	28.2
6	33	50	3	2.5	1.1	71.0	29.1

827

828 **Table 3**

Exp.	Water (wt%)	Mineral oil (wt%)	Added LA (wt%)	Added FA (wt%)	LA (g)	FA (g)	Δ_{LA} [a] (g)	Δ_{FA} [b] (g)	LA (g/L)	FA (g/L)
7	33	48.0	1.9	1.0	3.7	1.7	0.6	0.3	105.6	47.6
8	33	45.8	4.0	1.2	4.8	1.5	1.6	0.7	136.8	41.4
9	33	37.0	10.0	4.0	7.7	2.7	4.7	2.3	219.2	76.2

829

830 **Note a**: Δ_{LA} is the difference between the maximum amount of obtainable LA (evaluated on the
831 basis of the reference data of the Exp. 5, Table 2) and that effectively recovered.

832 **Note b**: Δ_{FA} is the difference between the maximum amount of obtainable FA (evaluated on the
833 basis of the reference data of the Exp. 5, Table 2) and that effectively recovered.

834
835

836 **Table 4**

Sample	Water content (wt%)	TAN (mg KOH/g)	Density (15°C) (Kg/m^3)	Viscosity (40°C) (mm^2/s)	Carbon residue (wt%)	Color
Starting mineral oil	<0.05	0.03	868.2	68.1	<0.1	L0.5
Recovered mineral oil	0.5	1.3	869.2	67.0	<0.1	L2

837

Figure S1: DSC curves of the starting and recovered (Exp. 5, Table 1) mineral oil, both acquired under air atmosphere.

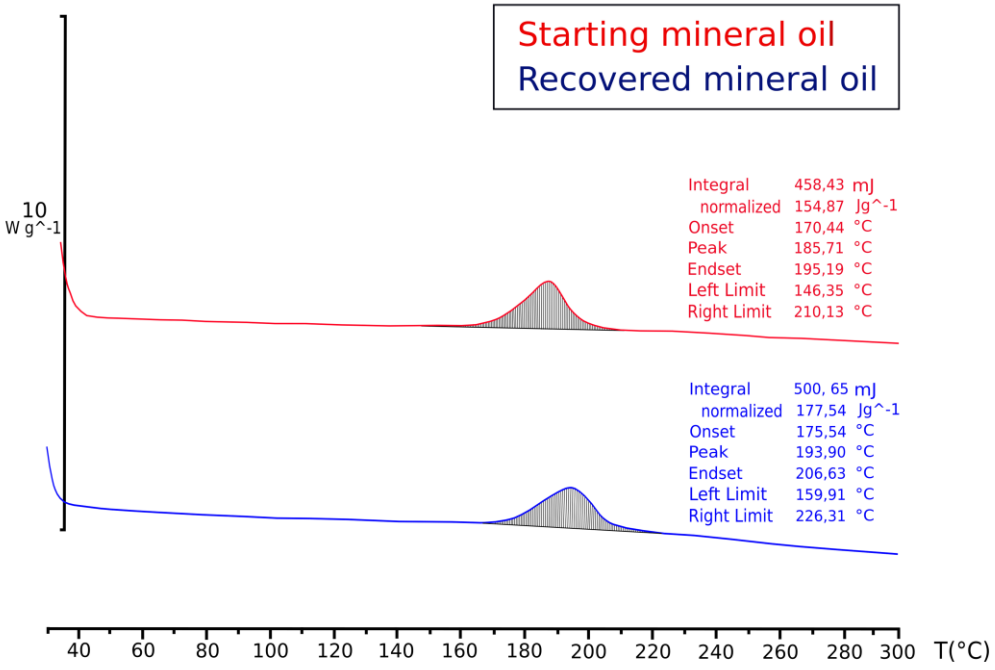

Figure S2: Distillation plots of the starting and recovered (Exp. 5, Table 1) mineral oil.

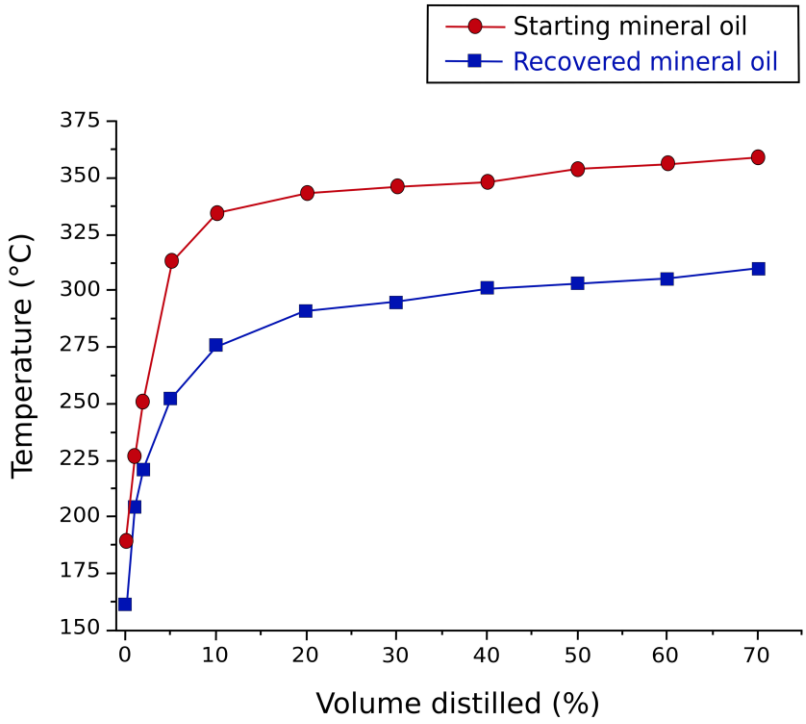

Figure S3: FT-IR spectra of the starting and recovered (Exp. 5, Table 1) mineral oil.

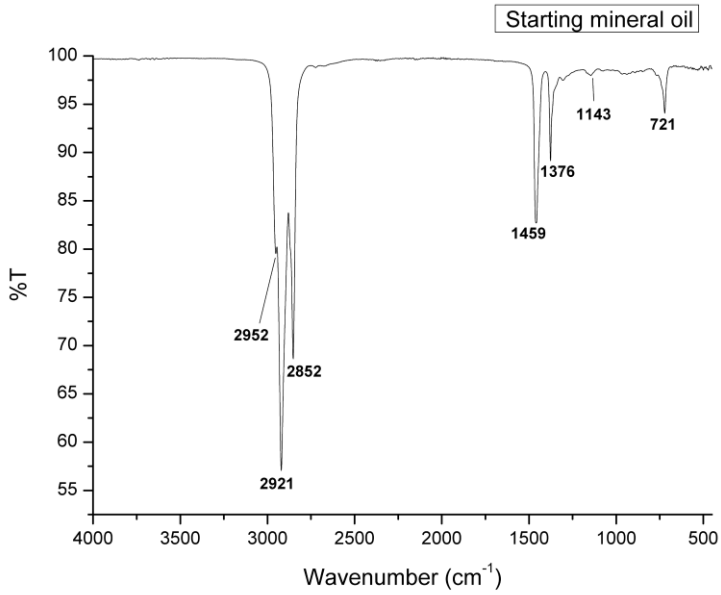

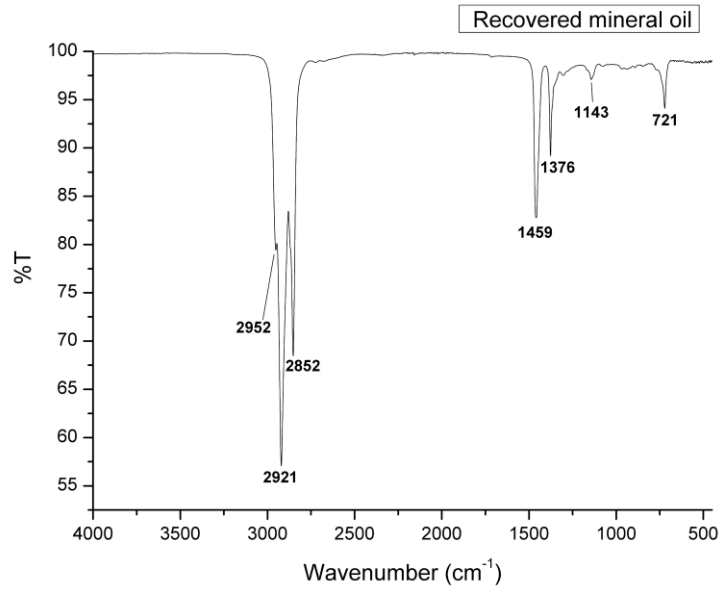

Figure S4: Total ion chromatogram (TIC) of the starting and recovered (Exp. 5, Table 1) mineral oil.

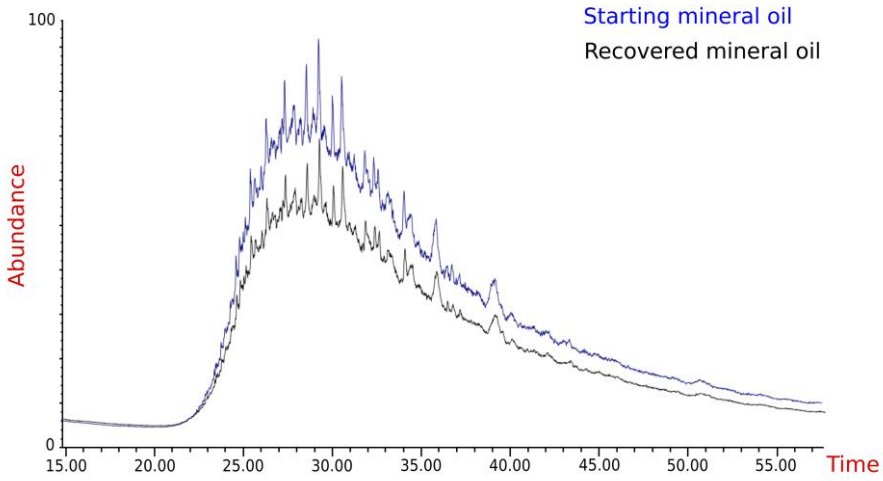

Figure S5: FT-IR spectra of the starting corn grain, monophasic- (Exp. 3, Table 1) and biphasic- (Exp. 5, Table 1) derived hydrochars, both recovered after LA production.